International Journal of
Molecular Sciences

MDPI

Article

Discovery of Novel Angiotensin-Converting Enzyme Inhibitory Peptides from *Todarodes pacificus* and Their Inhibitory Mechanism: In Silico and In Vitro Studies

Dingyi Yu [1], Cong Wang [2], Yufeng Song [1], Junxiang Zhu [1,*] and Xiaojun Zhang [1]

[1] Laboratory of Aquatic Product Processing and Quality Safety, Marine Fisheries Research Institute of Zhejiang, Zhoushan 316021, China
[2] Guangxi Key Laboratory of Chemistry and Engineering of Forest Products, Key Laboratory of Guangxi Colleges and Universities for Food Safety and Pharmaceutical Analytical Chemistry, School of Chemistry and Chemical Engineering, Guangxi University for Nationalities, Nanning 530006, China
* Correspondence: zhujunxiang89@126.com; Tel.: +86-188-5707-0076

Received: 19 August 2019; Accepted: 23 August 2019; Published: 26 August 2019

Abstract: In order to rapidly and efficiently excavate antihypertensive ingredients in *Todarodes pacificus*, its myosin heavy chain was hydrolyzed in silico and the angiotensin-converting enzyme (ACE) inhibitory peptides were predicted using integrated bioinformatics tools. The results showed the degree of hydrolysis (*DH*) theoretically achieved 56.8% when digested with papain, ficin, and prolyl endopeptidase (PREP), producing 126 ACE inhibitory peptides. By predicting the toxicity, allergenicity, gastrointestinal stability, and intestinal epithelial permeability, 30 peptides were finally screened, of which 21 had been reported and 9 were new. Moreover, the newly discovered peptides were synthesized to evaluate their in vitro ACE inhibition, showing Ile-Ile-Tyr and Asn-Pro-Pro-Lys had strong effects with a pIC_{50} of 4.58 and 4.41, respectively. Further, their interaction mechanisms and bonding configurations with ACE were explored by molecular simulation. The preferred conformation of Ile-Ile-Tyr and Asn-Pro-Pro-Lys located in ACE were successfully predicted using the appropriate docking parameters. The molecular dynamics (MD) result indicated that they bound tightly to the active site of ACE by means of coordination with Zn(II) and hydrogen bonding and hydrophobic interaction with the residues in the pockets of S_1 and S_2, resulting in stable complexes. In summary, this work proposed a strategy for screening and identifying antihypertensive peptides from *Todarodes pacificus*.

Keywords: ACE inhibitory peptides; *Todarodes pacificus*; molecular docking; molecular dynamics

1. Introduction

The angiotensin-converting enzyme (ACE) is a metal carboxypeptidase involved in the renin-angiotensin system, which not only controls blood pressure and electrolyte homeostasis, but also renal function and myocardial remodeling [1]. It can convert the hormone, angiotensin I, to angiotensin II, which is a potent vasoconstrictive peptide that causes blood vessels to narrow, resulting in an elevated blood pressure [2]. Therefore, ACE is a major target for lowering blood pressure and cardiovascular therapies, and its inhibition mainly leads to an overall antihypertensive effect.

ACE inhibitors, such as captopril, lisinopril, enalapril, and ramipril, have been on the market for more than three decades [1]. Although they have a tight binding pattern with the generic ACE active sites (Zn^{2+}, S_1, S_1', and S_2' pockets) and exhibit excellent cardiovascular therapeutic capabilities, ACE inhibitors have numerous side effects that can impair renal function, cause hyperkalemia [3],

and develop angioedema [4]. Recently, a population-based cohort study has revealed a relationship between the long-term use of ACE inhibitors and an increased risk of lung cancer [5]. Their side effects have focused researchers' interest on the search for alternative non-toxic and naturally generated peptides for controlling blood pressure.

Almost accompanied by the development of antihypertensive drugs, food-derived peptides with antihypertensive properties have received great attention over the past 30 years [6]. The antihypertensive effects of some well-known food-derived peptides are mediated by the inhibition of ACE. Compared with synthetic drugs, these natural ACE inhibitors are considered milder and safer. Many studies have focused on identifying new antihypertensive sequences from different food sources including milk, cheese, meat, various plants, and algae [6]. The tripeptide Ile-Pro-Pro and Val-Pro-Pro are released from β- and κ-casein produced by the fermentation of *Lactobacillus helveticus* and *Sacharomyces cerevisiae* on milk [7]. In the follow-up research progress, it was also confirmed that Ile-Pro-Pro and Val-Pro-Pro attenuate the development of hypertension in spontaneously hypertensive rats and has hypotensive properties in hypertensive subjects [8,9]. Other effective dipeptides or tripeptides, which were originally discovered from different edible sources, such as pork, chicken, and eggs, namely Ile-Trp, Leu-Trp, Phe-Pro, Phe-Tyr, Ile-Pro-Ala, Gly-Lys-Pro, Val-Tyr-Pro, Tyr-Pro, and Val-Tyr, also have the similar ACE inhibitory activity. In addition, the current studies have found ACE inhibitory peptides in a variety of marine protein resources, including fish, cephalopods, bivalves, algae, and some processing by-products [10–12]. The types and quantities of these proteins are much larger than terrestrial resources and have not been well developed. Furthermore, due to the specificity of the marine environment, their protein composition is different from terrestrial biological proteins. Therefore, proteins from the ocean can serve as a potential resource for excavating ACE inhibitory peptides.

The entire process of preparing bioactive peptides from natural proteins by conventional methods is cumbersome and time consuming, thus limiting and delaying their use in food and pharmaceutical applications [13]. Alternatively, with the development of computer technology and the popularity of various online databases, the prediction and identification of food protein-derived bioactive peptides has become a feasible method [14]. Through this approach in silico, researchers can release potential bioactive peptides from native protein sequences using one or several proteases of choice. Nowadays, some ACE inhibitory peptides have been identified from many plants and animals in silico, such as wheat [15], scallop [16], meat proteins [17], and common oat [18]. Although the screening process for these jobs varies from one standard to another, they all showed fast and efficient features.

In some Asian countries, *Todarodes pacificus* is a popular seafood because of its unique flavor and taste as well as its rich quality protein [19]. It is also one of the most important commercial cephalopods in China. A previous study demonstrated that the enzymatic hydrolysates of *Todarodes pacificus* exhibited higher antioxidant, tyrosinase inhibitory, and antielastase activities [20]. However, reports on the development of ACE inhibitory peptides in it are rare. So far, some literatures have only reported the extraction of ACE inhibitory peptides from the other species of squids. For instance, Lin et al. prepared the pepsin hydrolysate (<2 kDa) of *Dosidicus eschrichitii* with a great ACE inhibitory activity in vitro (IC_{50} = 0.33 mg/mL) [21]. Similarly, Alemán et al. reported the Alcalase hydrolysate from the inner and outer tunics of *Dosidicus gigas*, which was a potent ACE inhibitor (IC_{50} = 0.34 mg/mL) [22]. They also identified a new ACE inhibitory decapeptide (Gly-Arg-Gly-Ser-Val-Pro-Ala-Hyp-Gly-Pro) from the skin of *Dosidicus gigas* using pepsin and pancreatin digestion [23].

Therefore, the aim of this study was to explore the ACE inhibitory peptide from *Todarodes pacificus* based on a computer-assisted method. Plant proteases and prolyl endopeptidase (PREP) were selected to hydrolyze the myosin heavy chain of *Todarodes pacificus* in silico. Subsequently, the ACE inhibitory peptides therein were predicted and screened according to toxicity, allergenicity, gastrointestinal stability, and intestinal epithelial permeability. Among the peptides finally obtained, the ACE inhibitory activity of those newly discovered was evaluated by an in vitro method. Finally, the interactions mechanism between ACE and some new peptides were studied via molecular docking

and molecular dynamic (MD) simulation. This study is also an attempt to provide a protocol for the screening of ACE inhibitory peptides from food source proteins.

2. Results and Discussion

2.1. In Silico Hydrolysis of the Myosin Heavy Chain of Todarodes Pacificus

In the present study, two proteases derived from plants were used to hydrolyze the myosin heavy chain of *Todarodes pacificus* to produce ACE inhibitory peptides. They showed a wider specificity in comparison with other enzymes such as trypsin or pepsin, cleaving peptide bonds from multiple regions and frequently acting as both exo- and endopeptidase [24]. Besides, another enzyme PREP was selected for a supplementary hydrolysis after the action of plant proteases, which cleaved peptide bonds at the C-terminal side of Pro residues [25]. This hydrolysis specificity played a key role in the release of potent ACE inhibitory peptides, because a common feature of many potent ACE inhibitory sequences was the presence of Pro residues at one or more positions of the C-terminal region [26].

After digestion using the BIOPEP-UWM online [27], the simulated degree of hydrolysis (*DH)* of all enzymatic treatments is shown in Figure 1A. The result showed the papain, ficin, and their combination for the myosin heavy chain of *Todarodes pacificus* had the *DH* value of 38.1%, 42.9%, and 55.0%, respectively. After addition of PREP, the *DH* of each group increased, from 38.1% to 39.8% for papain, and from 42.9% to 47.9% for ficin. The *DH* of the complex enzymes consisting of papain, ficin and PREP was the highest in all enzyme treatments, reaching 56.8%. The above results indicated that the introduction of PREP was advantageous for the hydrolysis of the myosin heavy chain from *Todarodes pacificus*.

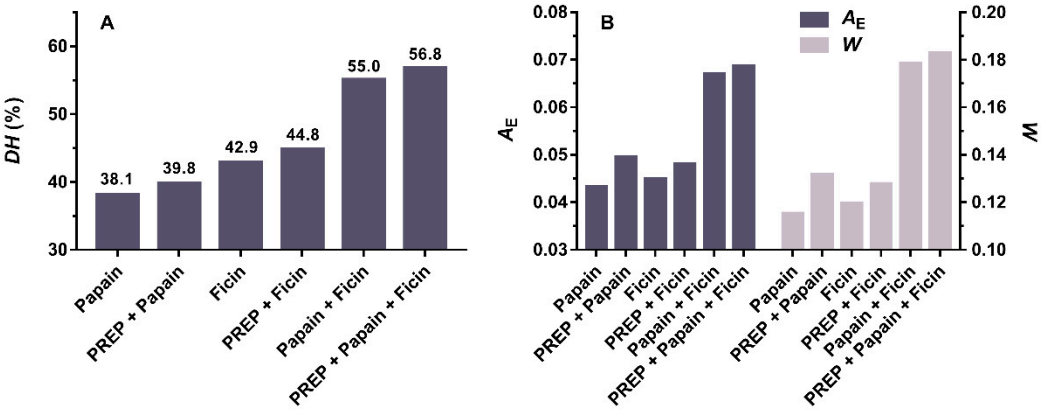

Figure 1. Degrees of hydrolysis (*DH*), release frequency (A_E), and relative frequency (*W*) of the myosin heavy chain of *Todarodes pacificus* digested by different enzymes. PREP represented prolyl endopeptidase.

Figure 1B showed the changes in frequency (A_E) and relative frequency (*W*) of the myosin heavy chain of *Todarodes pacificus* digested by different enzymes. A_E was the ratio of the number of ACE inhibitory peptides released by a given enzyme to the number of amino acid residues of the myosin [27]. *W* was the ratio of the number of ACE inhibitory peptides released by a given enzyme to the number of ACE inhibitory peptides in the myosin sequence [27]. They were all the quantitative parameters describing the predicted efficiency of proteolysis. The data in Figure 1B showed that the combination of papain and ficin significantly increased the A_E and *W* compared to hydrolysis using a single enzyme. Some previous studies indicated that papain and ficin were commonly used to produce antihypertensive peptides from food materials, such as oat [18], crude barley [28], and bovine fibrinogen [29]. In this study, papain and ficin were combined for enzymatic hydrolysis, indicating that it has a greater potential to release ACE inhibitory peptide than when they were used alone. After myosin underwent supplemental hydrolysis by PREP, the A_E and *W* further increased for all enzymatic treatments. For the case of single digestion by papain, supplementation with PREP increased A_E and

W by 14.3% and 14.1%, respectively, which was the largest increase in all hydrolysis groups. For the complex group of papain and ficin, the addition of PREP slightly enhanced the acquired frequency of ACE inhibitory peptides. The above results illustrated that the hydrolysis of squid myosin by papain and ficin together could enhance the effect of hydrolysis and improve the efficiency of release of potential antihypertensive peptides in the myosin heavy chain of *Todarodes pacificus*.

2.2. In Silico Prediction of ACE Inhibitory Peptides from Myosin Heavy Chain of Todarodes Pacificus

As discussed above, peptides with ACE inhibitory activity could be produced from the myosin heavy chain of *Todarodes pacificus* by two plant proteases and the supplemented PREP. However, since the ACE inhibitory peptides identified by the BIOPEP-UWM database were both dip- and tripeptides in this study, the ACE inhibitory tetra-, penta-, and hexapeptides obtained by digestion with papain, ficin, and PREP were further predicted using the AHTpin database [30]. Then, the number and type of ACE inhibiting peptides were statistically analyzed. As shown in Figure 2A, 117 and 105 ACE inhibitory peptides were produced by papain and ficin hydrolysis, respectively. Compared to the single enzyme treatment, the combination of papain and ficin yielded more ACE inhibitory peptides. When PREP was introduced into a single plant protease, the total number of ACE inhibitory peptides also increased, for papain from 117 to 129 and for ficin from 105 to 114. Additionally, comparing the hydrolysis of papain–ficin and papain–ficin–PREP, the number of ACE inhibitory peptides remained unchanged, both of which were 139 peptides. It was worth noting that after the myosin heavy chain of *Todarodes pacificus* was digested with papain and PREP, the number of di- and tripeptides increased by 10.2%, which was significantly higher than that of ficin and papain–ficin after adding PREP, well agreeing with the data of A_E and *W* (Figure 1B).

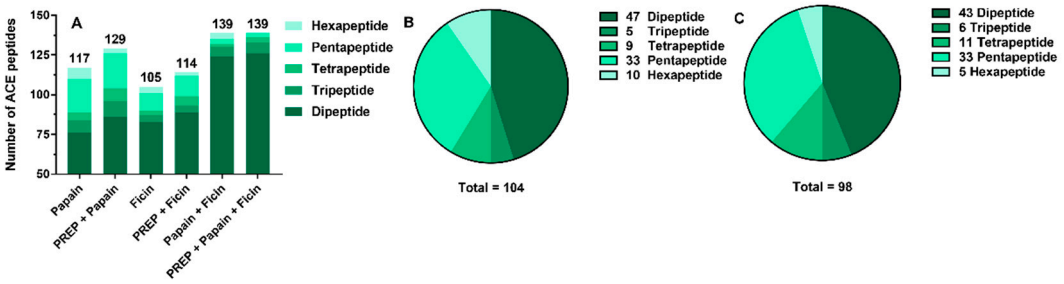

Figure 2. Number of ACE inhibitory peptides produced by different proteases in silico (**A**). Species of ACE inhibitory peptides released by hydrolysis using plant proteases without PREP (**B**) and with PREP (**C**) in silico. PREP was prolyl endopeptidase.

After merging the peptides with repeat sequences, the kinds of ACE inhibitory peptides obtained by the hydrolysis of plant proteases and plant proteases followed by PREP were analyzed and plotted in Figure 2B,C. The results showed that the addition of PREP to myosin digestion reduced the types of ACE inhibitory peptides, from 104 to 98. In detail, the di- and hexapeptides were reduced, and the tri- and tetrapeptides were increased.

The di- and tripeptides with ACE inhibitory activity generated by plant proteases without PREP are summarized in Table S1. They were all known peptides reported in some previous studies. Their pIC_{50} values were provided by the databases of AHTpin and BIOPEP-UWM, and their sources could be found in the databases of BIOPEP-UWM [27] and AHTPDB [31]. Among them, Met-Phe, Ile-Tyr, Asp-Gly, Glu-Tyr, Ser-Thr, and Val-Phe showed higher pIC_{50} values of 6.04, 5.68, 5.67, 5.57, 5.39, and 5.04, respectively. After the addition of PREP, as summarized in Table S2, the three groups of proteases produced 49 di- and tripeptides, of which the disappeared peptides were Ala-Phe, Glu-Trp, Glu-Tyr, Ile-Tyr, Met-Gly, Met-Tyr, Asn-Gly, Asn-Tyr, Pro-Gly, Pro-His, Pro-Leu, Pro-Pro-Lys, Val-Ala-Phe, Val-Glu, and Trp-Leu. The newly formed peptides were Ala-Ile-Pro, Ala-Pro, Ala-Val-Pro, Glu-Gly, Ile-Tyr, Lys-Pro, Met-Gly, Met-Tyr, Thr-Pro, and Val-Pro. Subsequently, the 52 tetra-, penta-, and

hexapeptides with ACE inhibitory activity in Table S3 were obtained by plant proteases without PREP and predicted by the AHTpin webserver [30]. Among them, Pro-Ile-Tyr-Thr, Glu-Lys-Ser-Arg, Ala-Ile-Asn-Pro-Tyr-Arg, Val-Ile-Gln-Tyr, Glu-Pro-Ile-Val-Lys, and Gln-Glu-Gln-Asp-His received higher scores of 1.06, 1.00, 0.99, 0.91, 0.87, and 0.86, respectively. After adding PREP, the proteases produced a total of 49 ACE inhibitory tetra-, penta-, and hexapeptides (Table S4). Among them, 19 peptides disappeared, and 16 peptides were newly produced, some of which had a C-terminal Pro residue, including Ala-Glu-Met-Pro-Pro, Ala-Ile-Asn-Pro, Cys-Ile-Ala-Ile-Asn-Pro, Cys-Ile-Ile-Pro, Ile-Glu-Lys-Pro, Asn-Ala-Ile-Pro, Asn-Cys-Trp-Val-Pro, Asn-Lys-Val-Lys-Pro, Gln-Cys-Asn-Pro, Gln-Met-Asn-Pro-Pro, and Ser-Lys-Glu-Pro. Moreover, Ile-Glu-Lys-Pro was the known ACE inhibitory peptide derived from catfish myofibrillar protein with an IC_{50} value of 2.1 μg/mL [32].

2.3. *In Silico Screening of ACE Inhibitory Peptides from Myosin Heavy Chain of Todarodes pacificus*

As described above, 104 and 98 ACE inhibitory peptides derived from *Todarodes pacificus* were obtained by plant proteases with and without PREP, respectively. Then, the peptides with the same sequence in the above two groups were merged, producing a total of 126 peptides for further screening based on the prediction of toxicity, allergenicity, gastrointestinal stability, and intestinal epithelial permeability.

As shown in Figure 3, the ACE inhibitory peptides that were resistant to the gastrointestinal environment were screened first. This was important because the active potential of peptides depended on their ability to access their target sites in an active form after passage through the gastrointestinal tract [6]. For example, Lys-Val-Leu-Pro-Val-Pro-Gln from the β-casein fragment showed a relatively weak ACE inhibitory activity in vitro while its antihypertensive effect in spontaneously hypertensive rats was effective. This was due to the conversion of Lys-Val-Leu-Pro-Val-Pro-Gln to Lys-Val-Leu-Pro-Val-Pro by pancreatin in the gastrointestinal tract, which was an active form in vivo [33]. The results in Figure 3 showed that 67 of the ACE inhibiting peptides were resistant to pepsin, trypsin, and chymotrypsin. The remaining 59 peptides were digested by the gastrointestinal proteases to form 40 new peptides. Together with the above-described 67 peptides resistant to gastrointestinal digestion, they were subjected to subsequent allergic prediction.

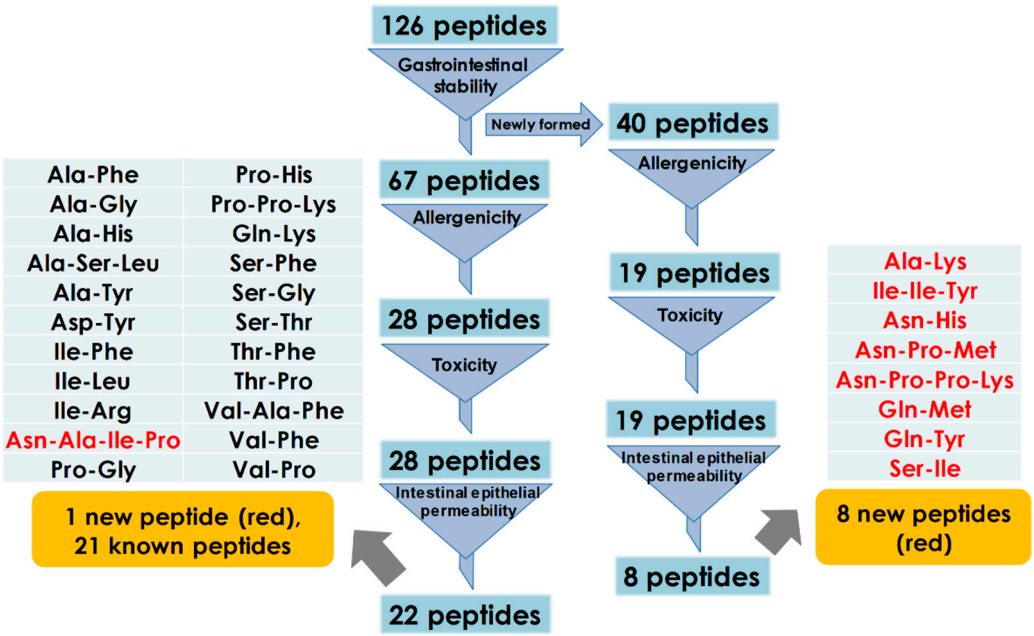

Figure 3. Screening process for ACE inhibitory peptides based on toxicity, allergenicity, gastrointestinal stability, and intestinal epithelial permeability.

Immunogenicity and toxicity remain the thorny issues in the development of peptide-based drugs. So, the potential allergenicity of the above gastrointestinally stable peptides was assessed using the AllerTOP tool [34], which is an alignment-free server for the in silico prediction of allergens based on the physicochemical properties of the amino acid sequence. As shown in Figure 3, a total of 47 peptides from myosin of *Todarodes pacificus* were predicted to be non-allergens. Next, these peptides were assessed for their potential toxicity by ToxinPred [35]. The results showed that all myosin hydrolysates were non-toxic, and no peptides with potential toxicity were predicted. Finally, the intestinal epithelial permeability of the selected peptides was evaluated using the 'the rule of 5', which predicted that poor absorption or permeation was more likely when there were more than five H-bond donors, ten H-bond acceptors, the molecular weight (MWT) was greater than five hundred, and the Log*P* was greater than five [36]. The results in Figure 3 indicated that only 30 ACE inhibitory peptides remained after the final permeability screening, of which 21 peptides were known antihypertensive peptides (Ala-Phe, Ala-Gly, Ala-His, Ala-Ser-Leu, Ala-Tyr, Asp-Tyr, Ile-Phe, Ile-Leu, Ile-Arg, Pro-Gly, Pro-His, Pro-Pro-Lys, Gln-Lys, Ser-Phe, Ser-Gly, Ser-Thr, Thr-Phe, Thr-Pro, Val-Ala-Phe, Val-Phe, and Val-Pro) and the remaining nine peptides were new peptides (Asn-Ala-Ile-Pro, Ala-Lys, Ile-Ile-Tyr, Asn-His, Asn-Pro-Met, Asn-Pro-Pro-Lys, Gln-Met, Gln-Tyr, and Ser-Ile). Finally, the predicted physicochemical properties of all the peptides are summarized in Tables S5 and S6, and the location of nine new ACE inhibitory peptides in the sequence of the myosin heavy chain of *Todarodes pacificus* was plotted in Figure S1.

2.4. ACE Inhibitory Activity of Peptides Derived from Todarodes Pacificus

As mentioned above, this study explored 21 known and 9 new ACE inhibitory peptides from the myosin heavy chain of *Todarodes pacificus*, which were non-toxic, non-allergic, and had good gastrointestinal stability and intestinal permeability. Among the known peptides, the one with the strongest ACE inhibitory capacity was the Ser-Thr (pIC_{50} = 5.39). This dipeptide was also found in marine shrimp *Acetes chinensis* fermented by *Lactobacillus fermentum* SM 605 [37]. Another dipeptide, Ala-Tyr, was observed to have a relatively good inhibitory effect on ACE (pIC_{50} = 4.85), which was also identified in the case of maize hydrolyzed using alcalase [38]. Moreover, in order to evaluate the ACE inhibitory ability of the newly discovered peptides, they were initially synthesized by a solid phase procedure and purified using a semi-preparative reversed-phase column. Then, their inhibitory rates were determined by an in vitro method, and the pIC_{50} values were calculated in Figure 4. The results indicated the tripeptide, Ile-Ile-Tyr, possessed the maximum pIC_{50} value of 4.58, and a sequence similar thereto has not been reported so far. The peptide with a second-best inhibitory effect on ACE was Asn-Pro-Pro-Lys (pIC_{50} = 4.41). The sequence of this tetrapeptide was reported to be similar to the ACE inhibitor from porcine skeletal muscle hydrolysate, namely Met-Asn-Pro-Pro-Lys [39], however its inhibition of ACE (pIC_{50} = 3.02) was significantly lower than Asn-Pro-Pro-Lys. These two new peptides had a great antihypertensive potential and their interaction with ACE needed a further study.

2.5. Inhibition Mechanisms of ACE by Ile-Ile-Tyr and Asn-Pro-Pro-Lys

As discussed above, this study explored the in vitro ACE inhibitory activity of nine new peptides, indicating that Ile-Ile-Tyr and Asn-Pro-Pro-Lys from the myosin heavy chain of *Todarodes pacificus* had antihypertensive potential. Thus, their interaction mechanism and bonding configurations with ACE was further studied using molecular docking and MD simulation.

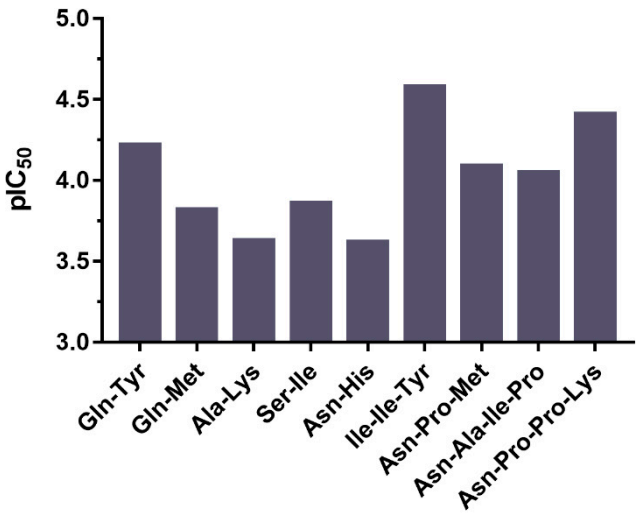

Figure 4. pIC_{50} values of nine new ACE inhibitory peptides from *Todarodes pacificus*.

2.5.1. Molecular Docking

The molecular docking could be used to predict the preferred orientation of these two peptides when they were bound to ACE to form a complex. Prior to the experiments, the docking parameters, including the maximum number of energy evaluations and the number of genetic algorithms, were studied and selected to better investigate the docking between ACE and its inhibitory peptide. The crystal structure of the human ACE in complex with lisinopril was used as the standard model [40]. The ligand, lisinopril, was extracted and re-docked to the active site of ACE. As shown in Figure 5A, in all docking experiments, the root mean square deviation (RMSD) difference between the docked lisinopril and the crystalline lisinopril was not significant. However, searching for 10 conformations of the docking procedure at a medium level of energy evaluations (2.5×10^6) resulted in poor precision with a relative standard deviation (RSD) of 26.8%. Similarly, the docking energy in Figure 5B indicated that the docking precision was also poor at a medium level of energy evaluations and 10 structural searches. The docking was repeated three times, one of which did not achieve an effective docking energy. For computational time consumption, the data in Figure 5C indicated that docking at a long level of energy assessment (2.5×10^7), or searching for 100 candidate structures, would take more than an hour to complete in our computer. At the medium level (2.5×10^6), the docking experiment examining 25 alternative conformations could be completed in 20 min. Moreover, the RSD of RMSD and docking energy under these conditions were small. Therefore, the maximum number of energy evaluations and the number of genetic algorithms were set to 2.5×10^6 and 25, respectively.

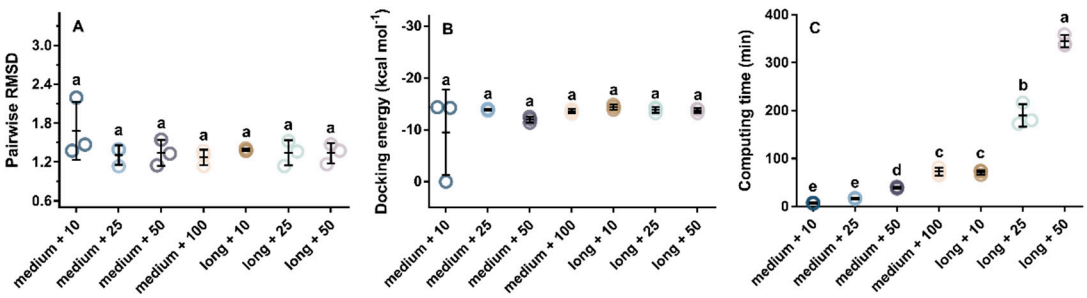

Figure 5. Effect of the maximum number of energy evaluations (medium and long) and the number of genetic algorithms (10, 25, 50, and 100) on the docking result of lisinopril with ACE: pairwise RMSD (**A**), docking energy (**B**), and computing time (**C**). RMSD was root mean square deviation.

Then, using the selected parameters, the docking of ACE with new inhibitory peptides was carried out. The data in Figure 6 showed that the docking energies of the test peptides were consistent with

their pIC_{50} to some extent. Among them, Ile-Ile-Tyr and Asn-Pro-Pro-Lys had lower docking energy with values of −10.87 and −10.74 kcal·mol^{-1}, respectively, which were also in line with their respective pIC_{50}.

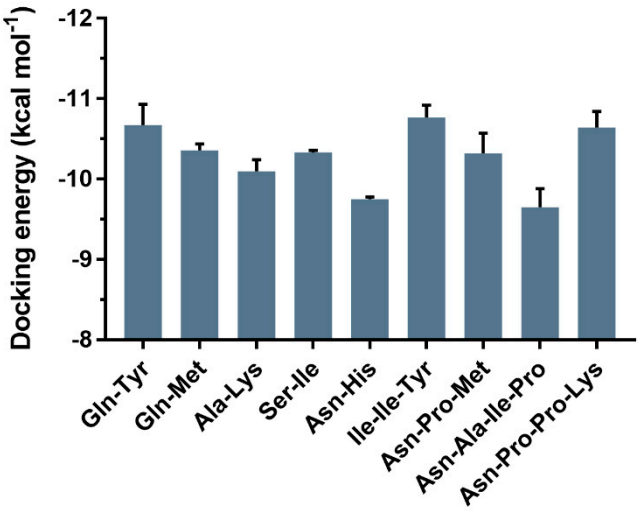

Figure 6. Docking energy of nine new ACE inhibitory peptides from *Todarodes pacificus*. Docking was performed according to the following parameters: maximum number of generations of 2.7×10^4, rate of gene mutation of 0.02, rate of crossover of 0.8, maximum number of energy evaluations of 2.5×10^6, number of genetic algorithms of 25.

The docking conformation in Figure 7 revealed that Ile-Ile-Tyr and Asn-Pro-Pro-Lys could be embedded in the S_1 hydrophobic pocket of ACE (Gln242, His344, His348, Glu372, Tyr484, and Glu345). The Asn-Pro-Pro-Lys was also close to Ala315 in the S_1 pocket, while Asn-Pro-Pro-Lys did not interact with this residue. For the S_2 pocket, Ile-Ile-Tyr was bound tightly to His314, Lys472, and His474 at this site, while Asn-Pro-Pro-Lys was only located near His314 and His474. In addition, Asn-Pro-Pro-Lys could interact with the Glu123 residue in the S_1' pocket. Further, analysis of the interaction between these two inhibitors and the surrounding amino acid residues at the active site of ACE indicated that there were three molecular forces involved in the stabilization of the peptides, including coordination, hydrogen bonding, and hydrophobic interaction. Figure 7 showed that Ile-Ile-Tyr and Asn-Pro-Pro-Lys could coordinate with the active site Zn(II) of ACE. The oxygen atom at the C-terminus of the peptide was in contact with Glu372, His344, and His348 by coordination interaction. As shown in Figure 7A, the Ile-Ile-Tyr formed two hydrogen bonds by reacting with the His348 and Asp346 residues of ACE. This tripeptide also entered the hydrophobic pocket of ACE and formed hydrophobic interactions with the Gln242, His314, Ser316, Ala317, Glu345, Glu372, Lys415, Lys472, Phe473, His474, Val479, Ser487, Phe488, and Gln491 residues. As shown in Figure 7B, the docking result of Asn-Pro-Pro-Lys and ACE was similar to those of the previous Ile-Ile-Tyr, forming two hydrogen bonds with the Glu337 and Glu345 residues. This tetrapeptide also interacted hydrophobically with the residues of Glu123, Asn238, Gln242, His314, Ala315, Ser316, Asp338, Val341, Phe473, His474, Val479, and Tyr484.

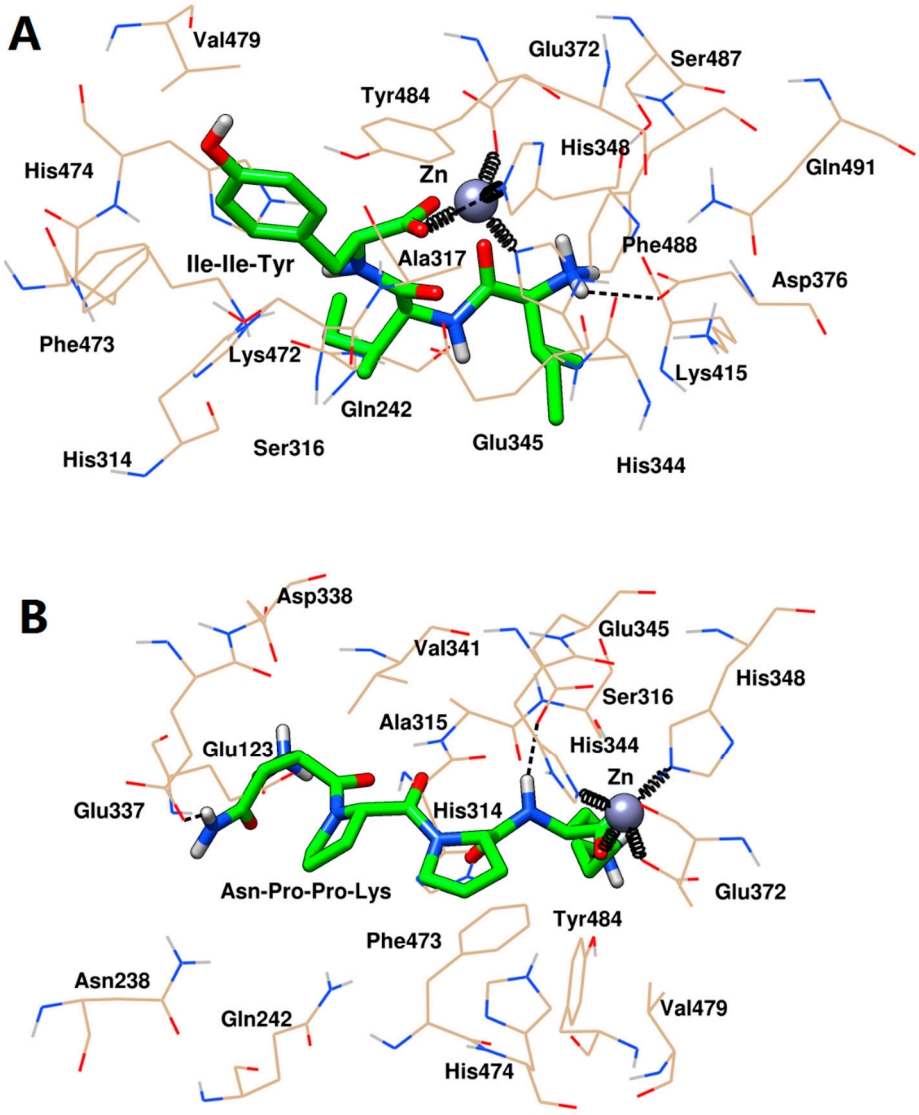

Figure 7. Docking conformation of Ile-Ile-Tyr (**A**) and Asn-Pro-Pro-Lys (**B**) with ACE. Gold lines represented the ACE residues involved in interacting with peptides. Green sticks represented the peptides. Grey sphere represented the Zn(II). Black dash lines represented the hydrogen bonds. Black springs represented the coordination bonds.

2.5.2. MD Simulation

Based on the docking conformation, MD simulation based on Ambertools with the metal center parameter builder (MCPB) was used to study the stable state of the complex of ACE with Ile-Ile-Tyr and Asn-Pro-Pro-Lys, and to further explore the interaction mechanism.

The variations of the RMSD regarding ACE with or without peptides are shown in Figure 8A. In general, if the RMSD value of a typical dynamic box fluctuated within 0.1 nm, the system could be considered to have reached a balanced steady state [41]. Obviously, the pure ACE and two ACE-peptide complexes were stable in 10 ns. Similar to RMSD, the root mean square fluctuation (RMSF) was used to analyze the difference in atomic position between a conformation of a biological macromolecule at a certain time and a reference conformation. The larger the RMSF of a residue of a protein, the higher its flexibility [42]. As shown in Figure 8B, ACE had five major flexible regions located at the 62–71, 115–117, 256–260, 306–312, 397–401, 434–437, 460–464, 503–506, and 577–579 residues, which were the peripheral random coil structures, away from the active center (Figure S2). After binding Ile-Ile-Tyr and Asn-Pro-Pro-Lys, ACE generally maintained a more stable conformation. The radius

of gyration (R_g) was used to describe the tightness of the protein structure. The greater the value, the higher the degree of protein unfolding [43]. The data in Figure 8C indicated that the average R_g of the ACE−peptide complex system was indistinguishable from the receptor ACE itself, indicating that the tightness of ACE did not change significantly after binding Ile-Ile-Tyr and Asn-Pro-Pro-Lys, and remained stable. To further realize the variation of R_g, the solvent accessible surface area (SASA) of free and peptide-binding ACE were studied. The SASA was defined as the surface area of the proteins that interacted with its solvent molecules, which had a certain correlation with the surface hydrophobicity of proteins [44]. The data in Figure 8D showed that the SASA of the system containing peptides was not significantly different from the pure ACE, indicating that the surface area of the ACE in contact with the solvent remained substantially the same before and after the complex formation with Ile-Ile-Tyr and Asn-Pro-Pro-Lys. This result also suggested the structure of ACE was stable after interaction with these two inhibitory peptides.

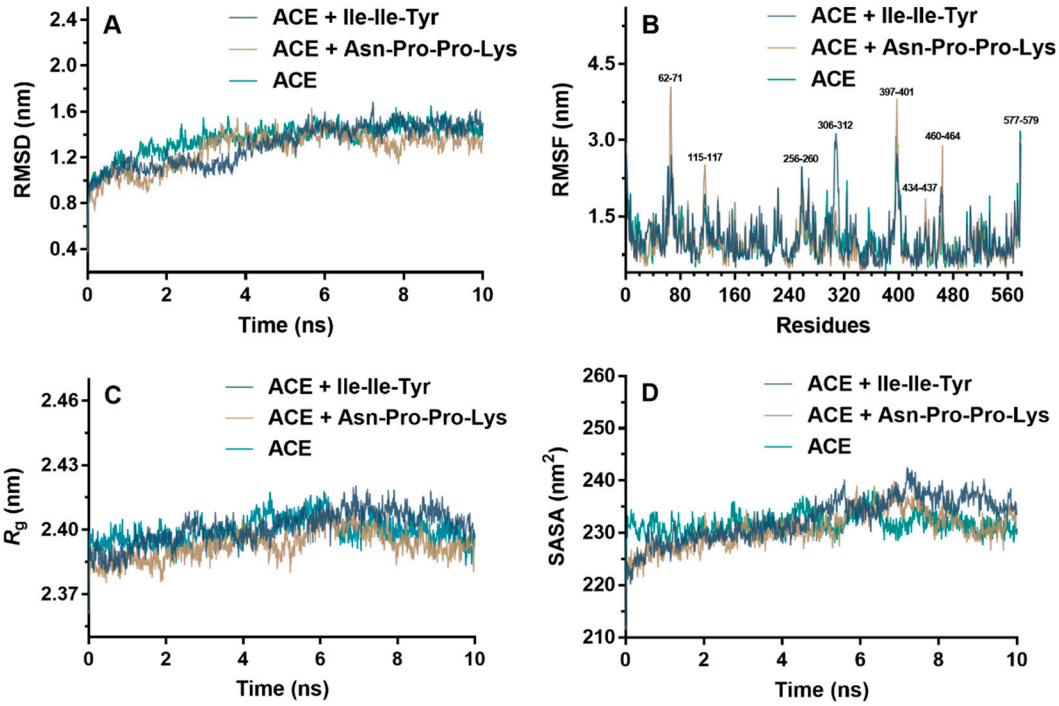

Figure 8. Molecular dynamics results of ACE with and without peptides Ile-Ile-Tyr and Asn-Pro-Pro-Lys: RMSD (**A**), RMSF (**B**), R_g (**C**), SASA (**D**). RMSD was root mean square deviation. RMSF was root mean square fluctuation. R_g was radius of gyration, SASA was solvent accessible surface area.

Figure 9A shows the hydrogen-bonding interactions between ACE and inhibitory peptides during the MD process. Throughout the simulation process, Asn-Pro-Pro-Lys can form more than three hydrogen bonds with ACE. However, for Ile-Ile-Tyr, the number of hydrogen bonds in the entire MD process can rarely exceed three. As shown in Figure 9B, the models of two hydrogen bonds were the stable conformations of ACE with Ile-Ile-Tyr and Asn-Pro-Pro-Lys, with frequencies of 86.3% and 39.5%, respectively. Additionally, in order to evaluate the coordination during MD, the distances between Zn(II) and its surrounding residues were calculated, including the His344, His348, Glu372 of ACE, and C-terminal residues (Tyr or Lys) of the inhibitory peptides.

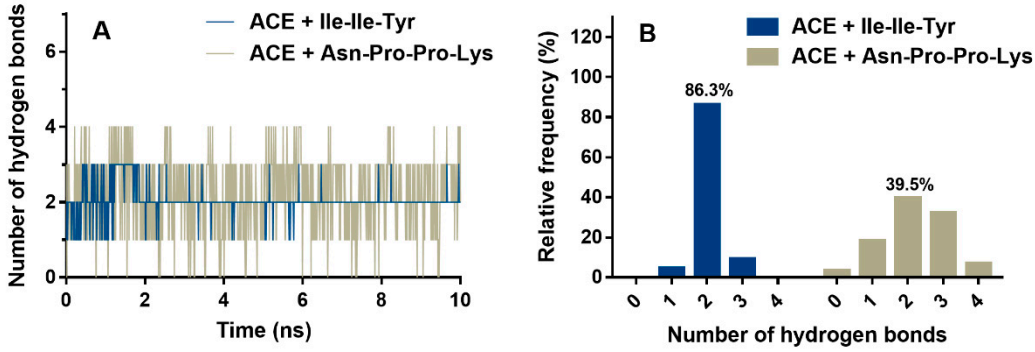

Figure 9. Number of hydrogen bonds between ACE and inhibitory peptides during molecular dynamics (**A**) and its frequency histogram (**B**).

Finally, the interaction between the two peptides and the active site of the target was further revealed by selecting the stable conformations of ACE with Ile-Ile-Tyr and Asn-Pro-Pro-Lys after the end of MD. As shown in Figure 11A, the His344, His348, and Glu372 residues in ACE and Ile-Ile-Tyr together formed coordinate bonds with Zn(II). Two hydrogen bonds were formed between the His474 and Asp376 residues in ACE and Ile-Ile-Tyr. Other amino acid residues, such as the His314, Ala315, Ser316, Val340, Val341, Lys415, Lys472, Phe473, Val479, Tyr484, and Phe488 residues, constituted a hydrophobic pocket surrounding the Ile-Ile-Tyr. As shown in Figure 11B, similarly, there was a coordination among the Asn-Pro-Pro-Lys, Zn(II), His344, His348, and Glu372 residues. Two hydrogen bonds were formed with the participation of the His314 and Asp388 residues. The other residues in ACE, including Glu123, Thr127, Trp240, Gln242, Ala315, Ser316, Ala317, Gln330, Asn335, Glu337, Glu345, Val341, Lys472, Phe473, His474, and Tyr484, could stabilize Asn-Pro-Pro-Lys by hydrophobic interactions. Moreover, these two peptides were observed to bind to the S_1 pocket of ACE (Ala315, His344, His348, Glu372, and Tyr484) upon forming the stable complexes. Similar to Figure 7, Asn-Pro-Pro-Lys could also interact with Glu345 in the S_1 pocket, while Ile-Ile-Tyr did not. After MD simulation, they were able to approach His314, Lys472, and His474 in the S_2 pocket, suggesting a tighter bonding configuration. Besides, Asn-Pro-Pro-Lys could also be close to Gln242 by hydrophobic force, which was another residue in the S_2 pocket. For the S_1' pocket, Ile-Ile-Tyr was alienated from it, but there was still an interaction between Asn-Pro-Pro-Lys and the Glu123 residue at this site.

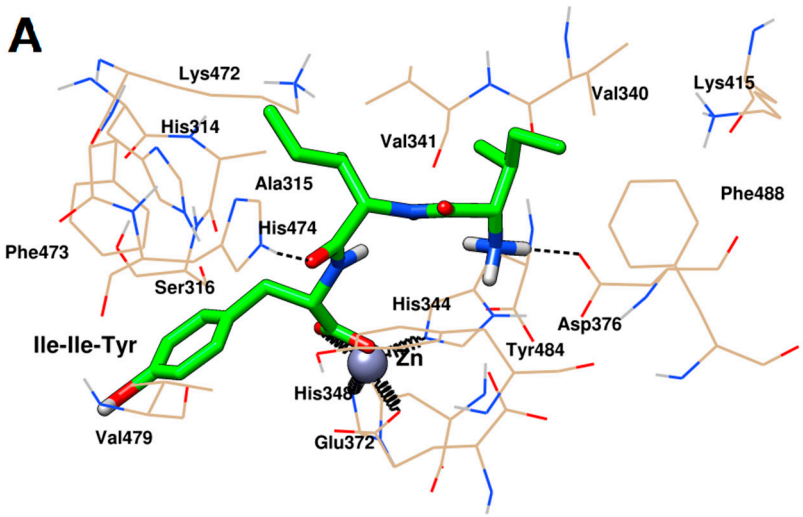

Figure 10. *Cont.*

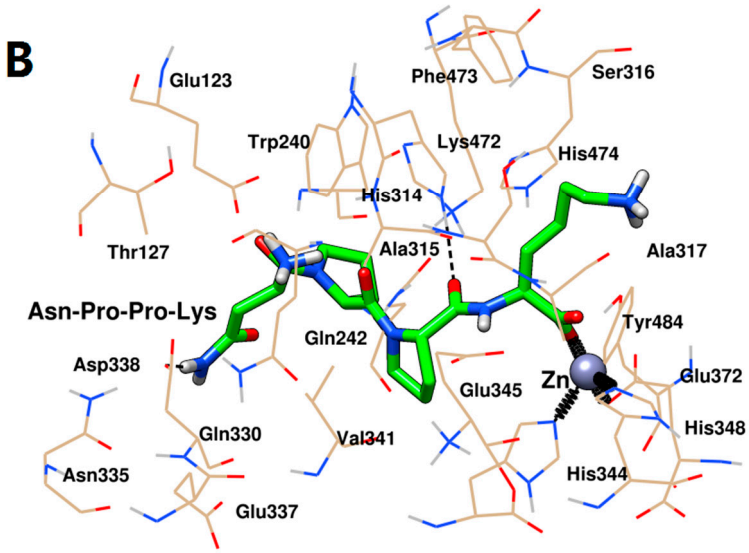

Figure 11. Molecular dynamics conformation of Ile-Ile-Tyr (**A**) and Asn-Pro-Pro-Lys (**B**) with ACE. Gold lines represented the ACE residues involved in interacting with peptides. Green sticks represented the peptides. Grey sphere represented the Zn(II). Black dash lines represented the hydrogen bonds. Black springs represented the coordination bonds.

3. Materials and Methods

3.1. Reagents

The tested peptides from t hmyosin heavy chain in *Todarodes pacificus* were provided by Anhui Guoping Pharmaceutical Co., Ltd. (Hefei, China). The ACE from rabbit lungs, hippuryl-histidyl-leucine (HHL), and hippuric acid (HA) were purchased from the Sigma Chemical Company (St. Louis, MO, USA). The solvents for high performance liquid chromatography (HPLC) including acetonitrile and trifluoroacetic acid (TFA) were provided by Merck (Darmstadt, Germany). All the other reagents and chemicals used were of analytical grade.

3.2. In Silico Hydrolysis

The myosin heavy chain (GenBank: ADU19853.1) from *Todarodes pacificus* was obtained from the NCBI protein database, available at https://www.ncbi.nlm.nih.gov/protein/. Then, it was hydrolyzed independently by the papain (EC 3.4.22.2), ficin (EC 3.4.22.3), and a combination of them using the BIOPEP-UWM database [27], available at http://www.uwm.edu.pl/biochemia/index.php/en/biopep. After hydrolysis by the plant proteases, the PREP (EC 3.4.21.26) was introduced and combined with the above three groups of proteases for supplemental digestion to produce a peptide with a C-terminal Pro residue. When performing this process, it was worth noting that the PREP only cleaved substrates whose sequences did not exceed 30 amino acids. Furthermore, when the Pro-Pro sequence was present at the C-terminus, its activity was blocked [45].

3.3. Prediction of ACE Inhibitory Peptides

The search of di- and tripeptides from myosin was performed using the database BIOPEP-UWM. Moreover, the *DH*, A_E, and *W* of release of fragments with a given type of activity by selected enzymes were also were calculated [27]. Furthermore, the tetra-, penta-, and hexapeptides with ACE inhibitory activity were predicted via the AHTpin database, available at http://crdd.osdd.net/raghava/ahtpin/index.php, which used support vector machine (SVM) regression and classification models based on amino acid composition prediction [30]. In this work, it was trained at a threshold of 0.0, i.e., any peptide predicted over a 0.0 threshold was labeled as bioactive.

3.4. In Silico Prediction of Physicochemical Properties of Peptides

Additional in silico analysis was performed to predict the toxicity, allergenicity, gastrointestinal stability, and intestinal epithelial permeability. For prediction of the toxic/non-toxic peptides, the ToxinPred tool was used based on the SVM module [35], available at http://crdd.osdd.net/raghava/toxinpred/. The SVM threshold was selected as 0.0. The allergenicity was predicted using the AllerTOP tool [34], available at http://www.ddg-pharmfac.net/AllerTOP/. This method was based on auto cross covariance (ACC) transformation of protein sequences into uniform equal-length vectors. The principal properties of the amino acids were represented by five E descriptors and the proteins are classified by the k-nearest neighbor algorithm (kNN, k = 1) based on a training set containing 2427 known allergens from different species and 2427 non-allergens. The resistance to digestion was predicted using pepsin (EC 3.4.21.1), trypsin (EC 3.4.21.4), and chymotrypsin (EC 3.4.21.2) in the ExPASy PeptideCutter database, available at https://web.expasy.org/peptide_cutter/. Finally, the intestinal epithelial permeability was assessed by 'the rule of 5', involving H-bond donors, H-bond acceptors, MWT, and Log*P* [36]. These parameters were calculated by XLOGP3 [46], available at http://www.sioc-ccbg.ac.cn/?p=42&software=xlogp3.

3.5. In Vitro ACE Inhibitory Activity

The ACE inhibitory activity analysis was performed based on Yu et al. with some modifications [16]. HHL was dissolved in 100 mM sodium borate buffer (pH 8.3) to achieve a final concentration of 5.8 mM. A reaction mixture containing 50 μL of ACE solution (100 mU/mL) and 100 μL of sample were pre-incubated at 37 °C for 5 min. Subsequently, 150 μL HHL was added and the mixture was incubated at 37 °C for 60 min. The reaction was terminated by the addition of 200 μL of 0.1 M HCl. The released HA was extracted by the addition of 1.0 mL ethyl acetate followed by centrifugation at 1000× *g* and 4 °C for 15 min. The upper layer was transferred into a new tube and purged with a stream of nitrogen. Then, 1 mL of deionized water was added. The amount of HA was determined via an ultra-performance liquid chromatography on a Waters Acquity UPLC BEH C18 column (1.7 μm, 2.1 mm × 100 mm). The dissolved samples were filtered through 0.22-μm syringe filters, and 10 μL were injected. The column was eluted with mobile phase (A) of 0.1% TFA in water and (B) of 25% acetonitrile at flow rates of 0.2 mL/min. The elution was observed at 228 nm. A series of standard HA solutions were prepared to construct a calibration curve. The degree of ACE inhibition was calculated as follows:

$$\text{ACE inhibition activity } (\%) = \frac{\text{A} - \text{B}}{\text{A}} \times 100\% \quad (1)$$

where *A* was the HA concentration of a reaction containing ACE without peptide, B was the HA concentration of a reaction in the presence of ACE and peptide. The IC_{50} was defined as the concentration of inhibitor required to inhibit 50% of the ACE activity.

3.6. Molecular Docking of ACE with Peptides

3.6.1. Selection of Docking Parameters

The AutoDock 4.2 package was used for the docking simulation based on a Lamarckian genetic algorithm [47]. Before the docking of our selected peptides with ACE, the conformation search parameters were optimized. Lisinopril from the crystal file (PDB 1O86) was selected as the experimental ligand. It was converted to a PDBQT file for later docking after merging non-polar hydrogens, assigning the polar hydrogens, and selecting the rotatable bonds. The zinc-centered map for ACE was calculated using an AutoGrid with 50 × 70 × 50 grid points of 0.375 Å spacing. The maximum number of generations was set to 2.7×10^4. The rate of gene mutation was set to 0.02. The rate of crossover was set to 0.8. The maximum number of energy evaluations was evaluated at the medium level (2.5×10^6) and the long level (2.5×10^7), and the number of genetic algorithms was examined at 10, 25, 50, and 100. The docking result was mainly evaluated by the RMSD difference between the docking structure

and the structure of lisinopril in the crystal ACE (PDB 1O86). Other indexes, such as the computing time and docking energy, were also considered.

3.6.2. Docking of ACE with Inhibitory Peptides

The models of Ile-Ile-Tyr and Asn-Pro-Pro-Lys for docking were generated by the Chimera program [48]. AutoDockTools 1.5.6rc3 was utilized to create the PDBQT format files by merging non-polar hydrogens, assigning the polar hydrogens, and selecting the rotatable bonds [47]. The AutoDock 4.2 program was used to determine the possible ACE–peptide conformation [47]. The processing parameters are those selected in Section 3.6.1. Finally, the Chimera package was used for the visualization of molecular docking results [48].

3.7. MD of ACE with Inhibitory Peptides

The initial conformations of ACE with peptides were obtained based on Section 3.6.2 and then simulated by all-atom MD using the AmberTools 18 package [49]. The Amber ff14SB all-atom force field was applied to simulate the complex of ACE with its peptides [50], which were solvated in a cubical periodic box with a 1.0 nm solute-wall distance using the transferable interatomic potential with three points model (TIP3P) water model. The coordinate bonds between Zn(II) and its surroundings were treated by the MCPB method [51], and the parameters of the amino acids coordinated with Zn(II) were obtained at the B3LYP/6-31G* level (Figure 12). Two phases of minimization were performed for the initial structures before the MD simulations. First, the solute atoms were restrained, and water molecules were minimized for 5000 steps with the steepest descent method followed by 5000 steps of conjugate gradient. Second, the unrestrained minimizations containing 5000 steps steepest descent and 5000 steps conjugate gradient of the whole systems were executed. The MD simulations were also set to two stages. First, the solutes were restrained, and the systems were slowly heated from 0 to 300 K over 50 ps. Then, non-restraint MD simulations at 300 K were performed for 10 ns. In these simulations, the SHAKE algorithm was applied to constrain covalent bonds. The MD time step was taken as 1 fs, and one snapshot was sampled every 10,000 steps (10 ps), thus 1000 conformations were obtained in each MD simulation. The Chimera package was used for the visualization of the MD results [48].

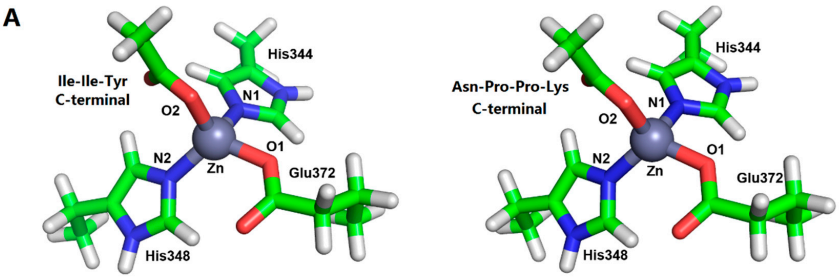

B

Asn-Pro-Pro-Lys	Angle (°)	Ile-Ile-Tyr	Angle (°)
O1-Zn-O2	113.415	O1-Zn-O2	113.351
O1-Zn-N1	92.28	O1-Zn-N1	92.306
O1-Zn-N2	116.966	O1-Zn-N2	117.002
O2-Zn-N1	112.208	O2-Zn-N1	112.21
O2-Zn-N2	109.789	O2-Zn-N2	109.782
N1-Zn-N2	111.172	N1-Zn-N2	111.185

Asn-Pro-Pro-Lys	Distance (Å)	Ile-Ile-Tyr	Distance (Å)
Zn-O1	1.795	Zn-O1	1.912
Zn-O2	1.706	Zn-O2	1.786
Zn-N1	1.993	Zn-N1	1.989
Zn-N2	1.908	Zn-N2	1.926
Asn-Pro-Pro-Lys	**Charge**	**Ile-Ile-Tyr**	**Charge**
Zn	+0.92	Zn	+0.93
O1	- 0.67	O1	- 0.67
O2	- 0.65	O2	- 0.65
N1	- 0.32	N1	- 0.33
N2	- 0.35	N2	- 0.35

Figure 12. Coordination conformation (**A**) and related parameters (**B**) between ACE active center Zn(II) and inhibitory peptides (Ile-Ile-Tyr and Asn-Pro-Pro-Lys).

4. Conclusions

In this work, nine novel ACE inhibitory peptides with short amino acids sequences were predicted and screened from *Todarodes pacificus* by an integrated bioinformatics approach. Among them, the tripeptide Ile-Ile-Tyr and tetrapeptide Asn-Pro-Pro-Lys exhibited strong inhibitory effects on ACE with pIC_{50} values of 4.58 and 4.41, respectively, which were also in line with their docking energies. Furthermore, MD simulation with the MCPB method showed that these two peptides could be deeply buried in the hydrophobic pockets of S_1 and S_2 of ACE, which were stabilized by coordination bonds with zinc ions and hydrogen bonding and hydrophobic interactions with surrounding residues. Thus, the present study demonstrated the potential of *Todarodes pacificus* as a suitable raw material for the industrial production of ACE-inhibitory peptides, which could be used to effectively treat hypertension.

Supplementary Materials: Supplementary materials can be found at http://www.mdpi.com/1422-0067/20/17/4159/s1.

Author Contributions: D.Y. conceived and designed the experiments, performed the experiments, analyzed the data, wrote the paper, prepared the figures and tables, and reviewed drafts of the paper. J.Z. conceived and designed the experiments, analyzed the data, contributed the tools in silico, and reviewed drafts of the paper. C.W., Y.S., and X.Z. reviewed drafts of the paper.

Funding: This research was funded by Zhejiang Province Public Welfare Technology Application Research Project (2018C37023) and Opening Project of Key Laboratory of Sustainable Utilization of Technology Research for Fishery Resource of Zhejiang Province.

Conflicts of Interest: The authors declare no conflict to interest.

References

1. Acharya, K.R.; Sturrock, E.D.; Riordan, J.F.; Ehlers, M.R. Ace revisited: A new target for structure-based drug design. *Nat. Rev. Drug Discov.* **2003**, *2*, 891–902. [CrossRef] [PubMed]
2. Murray, B.A.; FitzGerald, R.J. Angiotensin converting enzyme inhibitory peptides derived from food proteins: Biochemistry, bioactivity and production. *Curr. Pharm. Design* **2007**, *13*, 773–791. [CrossRef] [PubMed]
3. Cohn, J.N.; Kowey, P.R.; Whelton, P.K.; Prisant, L.M. New guidelines for potassium replacement in clinical practice: A contemporary review by the National Council on Potassium in Clinical Practice. *Arch. Intern. Med.* **2000**, *160*, 2429–2436. [CrossRef] [PubMed]
4. Baumgartner, L.J.; Morris, A.A.; Chapman, S.A. Angiotensin-converting enzyme inhibitor induced angioedema: Predictors of mechanical ventilation and treatment approaches. *Intens. Care. Med.* **2015**, *41*, 2233–2234. [CrossRef] [PubMed]
5. Hicks, B.M.; Filion, K.B.; Yin, H.; Sakr, L.; Udell, J.A.; Azoulay, L. Angiotensin converting enzyme inhibitors and risk of lung cancer: Population based cohort study. *BMJ Brit. Med. J.* **2018**, *363*, k4209. [CrossRef] [PubMed]
6. Miralles, B.; Amigo, L.; Recio, I. Critical review and perspectives on food-derived antihypertensive peptides. *J. Agric. Food Chem.* **2018**, *66*, 9384–9390. [CrossRef] [PubMed]
7. Korhonen, H.; Pihlanto, A. Bioactive peptides: Production and functionality. *Int. Dairy J.* **2006**, *16*, 945–960. [CrossRef]
8. Xu, J.Y.; Qin, L.Q.; Wang, P.Y.; Li, W.; Chang, C. Effect of milk tripeptides on blood pressure: A meta-analysis of randomized controlled trials. *Nutrition* **2008**, *24*, 933–940. [CrossRef] [PubMed]
9. Sipola, M.; Finckenberg, P.; Santisteban, J.; Korpela, R.; Vapaatalo, H.; Nurminen, M.L. Long-term intake of milk peptides attenuates development of hypertension in spontaneously hypertensive rats. *J. Physiol. Pharmacol.* **2001**, *52*, 745–754. [PubMed]
10. Byun, H.G.; Kim, S.K. Purification and characterization of angiotensin I converting enzyme (ACE) inhibitory peptides from Alaska pollack (*Theragra chalcogramma*) skin. *Process Biochem.* **2001**, *36*, 1155–1162. [CrossRef]
11. Ahn, C.B.; Jeon, Y.J.; Kim, Y.T.; Je, J.Y. Angiotensin I converting enzyme (ACE) inhibitory peptides from salmon byproduct protein hydrolysate by Alcalase hydrolysis. *Process Biochem.* **2012**, *47*, 2240–2245. [CrossRef]

12. Suetsuna, K.; Maekawa, K.; Chen, J.R. Antihypertensive effects of *Undaria pinnatifida* (wakame) peptide on blood pressure in spontaneously hypertensive rats. *J. Nutr. Biochem.* **2004**, *15*, 267–272. [CrossRef] [PubMed]
13. Udenigwe, C.C. Bioinformatics approaches, prospects and challenges of food bioactive peptide research. *Trends Food Sci. Tech.* **2014**, *36*, 137–143. [CrossRef]
14. Lacroix, I.M.; Li-Chan, E.C. Evaluation of the potential of dietary proteins as precursors of dipeptidyl peptidase (DPP)-IV inhibitors by an in silico approach. *J. Funct. Foods* **2012**, *4*, 403–422. [CrossRef]
15. Garg, S.; Apostolopoulos, V.; Nurgali, K.; Mishra, V.K. Evaluation of in silico approach for prediction of presence of opioid peptides in wheat. *J. Funct. Foods* **2018**, *41*, 34–40. [CrossRef]
16. Yu, Z.; Wu, S.; Zhao, W.; Ding, L.; Shiuan, D.; Chen, F.; Li, J.; Liu, J. Identification and the molecular mechanism of a novel myosin-derived ACE inhibitory peptide. *Food Funct.* **2018**, *9*, 364–370. [CrossRef] [PubMed]
17. Lafarga, T.; O'Connor, P.; Hayes, M. Identification of novel dipeptidyl peptidase-IV and angiotensin-I-converting enzyme inhibitory peptides from meat proteins using in silico analysis. *Peptides* **2014**, *59*, 53–62. [CrossRef] [PubMed]
18. Bleakley, S.; Hayes, M.; O'Shea, N.; Gallagher, E.; Lafarga, T. Predicted release and analysis of novel ACE-I, renin, and DPP-IV inhibitory peptides from common oat (*Avena sativa*) protein hydrolysates using in silico analysis. *Foods* **2017**, *6*, 108. [CrossRef]
19. Choi, S.; Puligundla, P.; Mok, C. Impact of corona discharge plasma treatment on microbial load and physicochemical and sensory characteristics of semi-dried squid (*Todarodes pacificus*). *Food Sci. Biotechnol.* **2017**, *26*, 1137–1144. [CrossRef]
20. Nam, K.A.; You, S.G.; Kim, S.M. Molecular and physical characteristics of squid (*Todarodes pacificus*) skin collagens and biological properties of their enzymatic hydrolysates. *J. Food Sci.* **2008**, *73*, C249–C255. [CrossRef]
21. Lin, L.; Lv, S.; Li, B. Angiotensin-I-converting enzyme (ACE)-inhibitory and antihypertensive properties of squid skin gelatin hydrolysates. *Food Chem.* **2012**, *131*, 225–230. [CrossRef]
22. Alemán, A.; Pérez-Santín, E.; Bordenave-Juchereau, S.; Arnaudin, I.; Gómez-Guillén, M.C.; Montero, P. Squid gelatin hydrolysates with antihypertensive, anticancer and antioxidant activity. *Food Res. Int.* **2011**, *44*, 1044–1051. [CrossRef]
23. Alemán, A.; Gómez-Guillén, M.C.; Montero, P. Identification of ace-inhibitory peptides from squid skin collagen after in vitro gastrointestinal digestion. *Food Res. Int.* **2013**, *54*, 790–795. [CrossRef]
24. Toldrá, F.; Reig, M.; Aristoy, M.C.; Mora, L. Generation of bioactive peptides during food processing. *Food Chem.* **2018**, *267*, 395–404. [CrossRef]
25. Norris, R.; O'Keeffe, M.B.; Poyarkov, A.; FitzGerald, R.J. Peptide identification and angiotensin converting enzyme (ACE) inhibitory activity in prolyl endoproteinase digests of bovine α_s-casein. *Food Chem.* **2015**, *188*, 210–217. [CrossRef]
26. Norris, R.; Poyarkov, A.; O'Keeffe, M.B.; FitzGerald, R.J. Characterisation of the hydrolytic specificity of *Aspergillus niger* derived prolyl endoproteinase on bovine β-casein and determination of ACE inhibitory activity. *Food Chem.* **2014**, *156*, 29–36. [CrossRef]
27. Iwaniak, A.; Minkiewicz, P.; Darewicz, M.; Sieniawski, K.; Starowicz, P. BIOPEP database of sensory peptides and amino acids. *Food Res. Int.* **2016**, *85*, 155–161. [CrossRef]
28. Gangopadhyay, N.; Wynne, K.; O'Connor, P.; Gallagher, E.; Brunton, N.P.; Rai, D.K.; Hayes, M. In silico and in vitro analyses of the angiotensin-I converting enzyme inhibitory activity of hydrolysates generated from crude barley (*Hordeum vulgare*) protein concentrates. *Food Chem.* **2016**, *203*, 367–374. [CrossRef]
29. Lafarga, T.; Rai, D.K.; O'Connor, P.; Hayes, M. A bovine fibrinogen-enriched fraction as a source of peptides with in vitro renin and angiotensin-I-converting enzyme inhibitory activities. *J. Agric. Food Chem.* **2015**, *63*, 8676–8684. [CrossRef]
30. Kumar, R.; Chaudhary, K.; Chauhan, J.S.; Nagpal, G.; Kumar, R.; Sharma, M.; Raghava, G.P. An in silico platform for predicting, screening and designing of antihypertensive peptides. *Sci. Rep-UK* **2015**, *5*, 12512. [CrossRef]

31. Kumar, R.; Chaudhary, K.; Sharma, M.; Nagpal, G.; Chauhan, J.S.; Singh, S.; Gautam, A.; Raghava, G.P. AHTPDB: A comprehensive platform for analysis and presentation of antihypertensive peptides. *Nucleic Acids Res.* **2014**, *43*, D956–D962. [CrossRef]
32. Ketnawa, S.; Rawdkuen, S. Purification and characterization of ACE inhibitory peptide from aquatic resources: A review. *Int. J. Pl. An and Env. Sci.* **2013**, *3*, 220–233.
33. Khedr, S.; Deussen, A.; Kopaliani, I.; Zatschler, B.; Martin, M. Effects of tryptophan-containing peptides on angiotensin-converting enzyme activity and vessel tone ex vivo and in vivo. *Eur. J. Nutr.* **2018**, *57*, 907–915. [CrossRef]
34. Dimitrov, I.; Bangov, I.; Flower, D.R.; Doytchinova, I. AllerTOP v.2—A server for in silico prediction of allergens. *J. Mol. Model.* **2014**, *20*, 2278. [CrossRef]
35. Gupta, S.; Kapoor, P.; Chaudhary, K.; Gautam, A.; Kumar, R.; Raghava, G.P.; Raghava, P.S.; Open Source Drug Discovery Consortium. In silico approach for predicting toxicity of peptides and proteins. *PLoS ONE* **2013**, *8*, e73957. [CrossRef]
36. Lipinski, C.A.; Lombardo, F.; Dominy, B.W.; Feeney, P.J. Experimental and computational approaches to estimate solubility and permeability in drug discovery and development settings. *Adv. Drug. Deliver. Rev.* **2012**, *64*, 4–17. [CrossRef]
37. Wang, Y.K.; He, H.L.; Chen, X.L.; Sun, C.Y.; Zhang, Y.Z.; Zhou, B.C. Production of novel angiotensin I-converting enzyme inhibitory peptides by fermentation of marine shrimp *Acetes chinensis* with *Lactobacillus fermentum* SM 605. *Appl. Microbiol. Biot.* **2008**, *79*, 785–791. [CrossRef]
38. Yang, Y.; Tao, G.; Liu, P.; Liu, J. Peptide with angiotensin I-converting enzyme inhibitory activity from hydrolyzed corn gluten meal. *J. Agric. Food Chem.* **2007**, *55*, 7891–7895. [CrossRef]
39. Arihara, K.; Nakashima, Y.; Mukai, T.; Ishikawa, S.; Itoh, M. Peptide inhibitors for angiotensin I-converting enzyme from enzymatic hydrolysates of porcine skeletal muscle proteins. *Meat Sci.* **2001**, *57*, 319–324. [CrossRef]
40. Natesh, R.; Schwager, S.L.; Sturrock, E.D.; Acharya, K.R. Crystal structure of the human angiotensin-converting enzyme–lisinopril complex. *Nature* **2003**, *421*, 551. [CrossRef]
41. Zhu, J.; Li, H.; Xu, Y.; Wang, D. Construction of fucoxanthin vector based on binding of whey protein isolate and its subsequent complex coacervation with lysozyme. *J. Agric. Food Chem.* **2019**, *67*, 2980–2990. [CrossRef]
42. Ning, X.; Zhang, Y.; Yuan, T.; Li, Q.; Tian, J.; Guan, W.; Liu, B.; Zhang, W.; Xu, X.; Zhang, Y. Enhanced thermostability of glucose oxidase through computer-aided molecular design. *Int. J. Mol. Sci.* **2018**, *19*, 425. [CrossRef]
43. Wang, Q.; Wang, Y.; Chen, G. Influence of secondary-structure folding on the mutually exclusive folding process of GL5/I27 protein: Evidence from molecular dynamics simulations. *Int. J. Mol. Sci.* **2016**, *17*, 1962. [CrossRef]
44. Ali, S.; Khan, F.I.; Mohammad, T.; Lan, D.; Hassan, M.; Wang, Y. Identification and evaluation of inhibitors of lipase from *Malassezia restricta* using virtual high-throughput screening and molecular dynamics studies. *Int. J. Mol. Sci.* **2019**, *20*, 884. [CrossRef]
45. Fülöp, V.; Böcskei, Z.; Polgár, L. Prolyl oligopeptidase: An unusual β-propeller domain regulates proteolysis. *Cell* **1998**, *94*, 161–170. [CrossRef]
46. Cheng, T.; Zhao, Y.; Li, X.; Lin, F.; Xu, Y.; Zhang, X.; Li, Y.; Wang, R.; Lai, L. Computation of octanol−water partition coefficients by guiding an additive model with knowledge. *J. Chem. Inf. Model.* **2007**, *47*, 2140–2148. [CrossRef]
47. Morris, G.M.; Huey, R.; Lindstrom, W.; Sanner, M.F.; Belew, R.K.; Goodsell, D.S.; Olson, A.J. AutoDock4 and AutoDockTools4: Automated docking with selective receptor flexibility. *J. Comput. Chem.* **2009**, *30*, 2785–2791. [CrossRef]
48. Pettersen, E.F.; Goddard, T.D.; Huang, C.C.; Couch, G.S.; Greenblatt, D.M.; Meng, E.C.; Ferrin, T.E. UCSF Chimera—a visualization system for exploratory research and analysis. *J. Comput. Chem.* **2004**, *25*, 1605–1612. [CrossRef]
49. Case, D.; Ben-Shalom, I.; Brozell, B.; Cerutti, D.; Cheatham, T.; Cruzeiro, V.; Darden, T.; Duke, R.; Ghoreishi, D.; Gilson, M.; et al. *AMBER 2018*; University of California: San Francisco, CA, USA, 2018.

50. Maier, J.A.; Martinez, C.; Kasavajhala, K.; Wickstrom, L.; Hauser, K.E.; Simmerling, C. ff14SB: Improving the accuracy of protein side chain and backbone parameters from ff99SB. *J. Chem. Theory Comput.* **2015**, *11*, 3696–3713. [CrossRef]
51. Li, P.; Merz, K.M., Jr. MCPB.py: A python based metal center parameter builder. *J. Chem. Inf. Model.* **2016**, *56*, 599–604. [CrossRef]

© 2019 by the authors. Licensee MDPI, Basel, Switzerland. This article is an open access article distributed under the terms and conditions of the Creative Commons Attribution (CC BY) license (http://creativecommons.org/licenses/by/4.0/).

Supplementary Materials

Table S1 ACE inhibitory di- and tripeptides released from the myosin heavy chain of *Todarodes pacificus* hydrolyzed by papain, ficin and papain−ficin *in silico*

Peptide	pIC_{50}[a]	Source[b]	Peptide	pIC_{50}[a]	Source[b]
AF	3.78	Soybean	NF	4.33	Garlic (*Allium sativum* L)
AG	2.60	Carp parvalbumin	NG	1.92	Chicken (*Gallus gallus*)
AH	3.28	Sweet potato tuber	NK	3.09	Pork sarcoplasmic proteins
AR	4.02	Pork skeletal muscle	NY	4.49	Garlic (*Allium sativum* L)
AY	4.85	Soybean	PG	1.77	Pork sarcoplasmic proteins
DG	5.67	Soybean	PH	/	Pork sarcoplasmic proteins
DY	4.00	Oyster protein hydrolysate	PL	3.47	Pork sarcoplasmic proteins
EG	2.00	Pork sarcoplasmic proteins	QG	2.13	Carp parvalbumin
EI	/	Chicken (*Gallus gallus*)	QK	3.05	Pork sarcoplasmic proteins
EK	/	Chicken (*Gallus gallus*)	SF	3.89	Garlic (*Allium sativum L*)
EW	3.86	Chicken (*Gallus gallus*)	SG	2.07	Carp parvalbumin
EY	5.57	Shark meat	ST	5.39	Marine shrimp (*Acetes chinensis*)
HL	2.49	Pork sarcoplasmic proteins	TF	4.74	Rapeseed proteins
IF	4.18	Soybean sauce	VE	/	Pork sarcoplasmic proteins
IG	2.92	Carp parvalbumin	VF	5.04	Wakame (*Undaria pinnatifida*)
IL	4.26	/	VG	2.96	Soybean
IR	3.16	Bovine β-lactoglobulin	VK	4.89	Carp parvalbumin
IY	5.68	Dried bonito	VR	4.28	Ovine milk proteins
KF	4.55	Wakame (*Undaria pinnatifida*)	WL	4.52	Soybean
KG	2.49	Pork sarcoplasmic proteins	YG	2.82	Pork sarcoplasmic proteins
KL	4.30	Carp parvalbumin	YL	4.09	Sardine muscle (*Sardina pilchardus*)
KR	3.42	Pork sarcoplasmic proteins	AEL	4.24	Algae (*Chlorella vulgaris*)
MF	6.04	Shark	ASL	3.99	Silkworm pupa (*Bombyx mori*)
MG	2.32	Chicken (*Gallus gallus*)	NKL	4.06	Bovine β-casein
MM	3.26	Poultry protein	PPK	3.00	Porcine skeletal muscle protein
MY	3.71	Carp parvalbumin	VAF	4.45	Algae (*Spirulina platensis*)

[a] pIC_{50} is derived from the AHTpin and BIOPEP-UWM databases

[b] Sources of peptides are provided by the BIOPEP-UWM and AHTPDB databases

Table S2 ACE inhibitory di- and tripeptides released from the myosin heavy chain of *Todarodes pacificus* hydrolyzed by papain−prolyl endopeptidase, ficin−prolyl endopeptidase, and papain−ficin−prolyl endopeptidase *in silico*

Peptide	pIC_{50}[a]	Source[b]	Peptide	pIC_{50}[a]	Source[b]
AF	3.78	Soybean	MY	3.71	Sardine muscle (*Sardina pilchardus*)
AG	2.60	Carp parvalbumin	NF	4.33	Garlic (*Allium sativum L*)
AH	3.28	Sweet potato tuber	NG	1.92	Chicken (*Gallus gallus*)
AP	4.54	Atlantic salmon	NK	3.09	Pork sarcoplasmic proteins
AR	4.02	Algae (*Chlorella vulgaris*)	QG	2.13	Carp parvalbumin
AY	4.85	Soybean	QK	3.05	Pork sarcoplasmic proteins
DG	5.67	Soybean	SF	3.89	Garlic (*Allium sativum L*)
DY	4.00	Oyster protein hydrolysate	SG	2.07	Carp parvalbumin
EG	2.00	Pork sarcoplasmic proteins	ST	5.39	Marine shrimp (*Acetes chinensis*)
EI	/	Chicken (*Gallus gallus*)	TF	4.74	Rapeseed proteins
EK	/	Chicken (*Gallus gallus*)	TP	3.54	Anchovy sauce
HL	2.49	Pork sarcoplasmic proteins	VF	5.04	Wakame (*Undaria pinnatifida*)
IF	4.18	Soybean sauce	VG	2.96	Soybean
IG	2.92	Carp parvalbumin	VK	4.89	Carp parvalbumin
IL	4.26	/	VP	3.38	Soybean
IR	3.16	Bovine β-lactoglobulin	VR	4.78	Ovine milk proteins
IY	5.68	Dried bonito	YG	2.82	Pork sarcoplasmic proteins
KF	4.55	Wakame (*Undaria pinnatifida*)	YL	4.09	Carp parvalbumin
KG	2.49	Pork sarcoplasmic proteins	AEL	4.24	Algae (*Chlorella vulgaris*)
KL	4.30	Carp parvalbumin	AIP	3.46	Bovine β-lactoglobulin
KP	4.66	Anchovy sauce	ASL	3.99	Silkworm pupa (*Bombyx mori*)
KR	3.42	Pork sarcoplasmic proteins	AVP	3.47	Bovine β-casein
MF	6.04	Shark	NKL	4.06	Bovine β-casein
MG	2.32	Chicken (*Gallus gallus*)	VAF	4.45	Algae (*Spirulina platensis*)
MM	3.26	Poultry protein			

[a] pIC_{50} is derived from the AHTpin and BIOPEP-UWM databases

[b] Sources of peptides are provided by the BIOPEP-UWM and AHTPDB databases

Table S3 ACE inhibitory tetra-, penta-, and hexapeptides released from the myosin heavy chain of *Todarodes pacificus* hydrolyzed by papain, ficin and papain−ficin *in silico*

Peptide	SVM score[a]	Peptide	SVM score[a]	Peptide	SVM score[a]
ADIKEL	0.10	EKKIR	0.36	PIYT	1.06
AEKV	0.05	EKSR	1.00	PPEPDT	0.27
AEMPPH	0.34	EMKWK	0.48	QCNPVL	0.23
AEQEK	0.37	ENAQK	0.35	QDHEN	0.30
AETQK	0.25	EPIVK	0.87	QEQDH	0.86
AINPY	0.71	EQEEY	0.38	QESKT	0.14
AINPYR	0.99	HIKEL	0.68	QKNDL	0.32
AIPS	0.57	HKESL	0.39	QKVKSR	0.16
AKEHF	0.33	IIYSEF	0.14	QMNPPK	0.23
AKNR	0.21	IKKKL	0.59	QVKEL	0.75
AVPDPG	0.37	KKKKG	0.40	SKVEK	0.19
AYKKL	0.77	KNPMF	0.20	VDKYR	0.28
CEQMR	0.46	KNYER	0.55	VIQY	0.91
CIEAH	0.52	MQQK	0.32	VQQEL	0.71
CINYT	0.56	NHHMF	0.14	YDNHL	0.34
DNQIK	0.22	NKVKPL	0.02	YESG	0.70
DQIDQL	0.19	NPMF	0.54		
EEVQK	0.65	NYHIF	0.51		

[a] SVM score above 0 means the peptide is predicted to be antihypertensive using the AHTpin database

Table S4 ACE inhibitory tetra-, penta-, and hexapeptides released from *Todarodes pacificus* myosin hydrolyzed by papain−prolyl endopeptidase, ficin−prolyl endopeptidase and papain−ficin−prolyl endopeptidase *in silico*

Peptide	SVM score[a]	Peptide	SVM score[a]	Peptide	SVM score[a]
ADIKEL	0.10	ENAQK	0.35	QDHEN	0.30
AEMPP	0.50	EQEEY	0.38	QEQDH	0.86
AEQEK	0.37	EYVT	0.05	QESKT	0.14
AETQK	0.25	HIKEL	0.68	QKNDL	0.32
AINP	0.34	IEKP	0.50	QKVKSR	0.16
AKEHF	0.33	IIYSEF	0.14	QMNPP	0.98
AYKKL	0.77	IKKKL	0.59	QVKEL	0.75
CEQMR	0.46	KIKVG	0.33	QYML	1.06
CIAINP	0.28	KKKKG	0.40	SKEP	0.32
CIEAH	0.52	KNYER	0.55	SKVEK	0.19
CIIP	0.62	MQQK	0.32	VDKYR	0.28
CINYT	0.56	NAIP	0.34	VIQY	0.91
DNQIK	0.22	NCWVP	1.30	VQQEL	0.71
DQIDQL	0.19	NHHMF	0.14	YDNHL	0.34
EEVQK	0.65	NKVKP	1.20	YSIL	0.21
EKKIR	0.36	NYHIF	0.51		
EMKWK	0.48	QCNP	0.78		

[a] SVM score above 0 means the peptide is predicted to be antihypertensive using the AHTpin database

Table S5 Predicted toxicity, allergenicity, gastrointestinal stability, and intestinal epithelial permeability of selected peptides

Peptide	Toxicity	Allergenicity	CLog*P*	H-bond donors	H-bond acceptors	MWT	Gastrointestinal stability
AF	Non	Non	−2.47	3	3	236.3	Good
AG	Non	Non	−3.65	3	3	146.1	Good
AH	Non	Non	−3.84	4	4	226.2	Good
AL	Non	Allergen	−2.78	3	3	202.3	Good
AP	Non	Allergen	−2.71	2	3	186.2	Good
AR	Non	Allergen	−4.98	5	3	245.3	Good
AY	Non	Non	−3.48	4	4	252.3	Good
DG	Non	Allergen	−4.52	4	5	190.2	Good
DY	Non	Non	−4.35	5	6	296.3	Good
EG	Non	Allergen	−2.66	4	5	204.2	Good
EI	Non	Allergen	−3.47	4	5	260.3	Good
EK	Non	Allergen	−6.28	5	5	275.3	Good
EW	Non	Allergen	−2.65	5	5	333.3	Good
EY	Non	Allergen	−3.77	5	6	310.3	Good
HL	Non	Non	−2.17	3	4	268.3	H-L
IF	Non	Non	−1.81	3	3	278.3	Good
IG	Non	Allergen	−2.50	3	3	188.2	Good
IL	Non	Non	−1.71	3	3	244.3	Good
IR	Non	Non	−3.86	5	3	287.4	Good
IY	Non	Allergen	−2.16	4	4	294.3	Good
KF	Non	Allergen	−2.71	4	3	293.4	K-F
KG	Non	Non	−3.89	4	3	203.2	K-G
KL	Non	Non	−3.02	4	3	259.3	K-L
KP	Non	Non	−3.32	3	3	243.3	K-P
KR	Non	Non	−4.31	6	3	302.4	K-R
MF	Non	Allergen	−1.67	3	3	296.4	M-F
MG	Non	Non	−3.01	3	3	206.3	M-G
MM	Non	Non	−2.55	3	3	280.4	M-M
MY	Non	Allergen	−2.03	4	4	312.4	Good
NF	Non	Allergen	−3.99	4	4	279.3	N-F
NG	Non	Allergen	−5.17	4	4	189.2	Good
NK	Non	Allergen	−5.01	5	4	260.3	Good
NY	Non	Allergen	−5.00	5	5	295.3	Good
PG	Non	Non	−3.81	3	3	172.2	Good
PH	Non	Non	−2.80	4	5	349.4	Good
PL	Non	Allergen	−2.41	3	3	228.3	Good
QG	Non	Allergen	−4.52	4	4	203.2	Good
QK	Non	Non	−4.65	5	4	274.3	Good
SF	Non	Non	−3.52	4	4	252.3	Good

SG	Non	Non	−4.70	4	4	162.1	Good
ST	Non	Non	−4.92	5	5	206.2	Good
TF	Non	Non	−3.09	4	4	266.3	Good
TP	Non	Non	−3.33	3	4	216.2	Good
VE	Non	Allergen	−3.90	4	5	246.3	Good
VF	Non	Non	−2.16	3	3	264.3	Good
VG	Non	Allergen	−2.69	3	3	174.2	Good
VK	Non	Allergen	−3.63	4	3	245.3	Good
VP	Non	Non	−2.15	2	3	214.3	Good
VR	Non	Allergen	−4.21	5	3	273.3	Good
WL	Non	Non	−0.73	4	3	317.4	W-L
YG	Non	Allergen	−2.86	4	4	238.2	Y-G
YL	Non	Allergen	−1.75	4	4	294.3	Y-L
AEL	Non	Allergen	−3.86	5	6	331.4	Good
AIP	Non	Allergen	−2.04	3	4	299.4	Good
ASL	Non	Non	−3.67	5	5	289.3	Good
AVP	Non	Allergen	−3.26	3	4	285.3	Good
NKL	Non	Non	−3.92	6	5	373.4	NK-L
PPK	Non	Non	−2.80	4	4	340.4	Good
VAF	Non	Non	−1.66	4	4	335.4	Good
AEKV	Non	Non	−7.41	7	7	445.5	AE-K-V
AINP	Non	Allergen	−5.34	5	6	413.5	Good
AIPS	Non	Allergen	−4.89	5	6	386.4	Good
AKNR	Non	Non	−6.33	9	6	487.6	AK-NR
CIIP	Non	Allergen	−2.58	4	5	444.6	Good
EKSR	Non	Non	−8.66	10	8	518.6	EK-SR
EYVT	Non	Non	−3.51	8	9	510.5	EY-VT
IEKP	Non	Non	−6.85	6	7	485.6	Good
MQQK	Non	Allergen	−5.68	8	7	533.6	M-QQK
NAIP	Non	Non	−5.34	5	6	413.5	Good
NPMF	Non	Allergen	−4.17	5	6	507.6	NPM-F
PIYT	Non	Non	−0.51	6	6	504.6	PIY-T
QCNP	Non	Non	−7.90	6	7	460.5	Good
QYML	Non	Non	−3.44	7	7	553.7	QY-M-L
SKEP	Non	Allergen	−9.22	7	8	459.5	SK-EP
VIQY	Non	Non	−3.57	7	7	521.6	Good
YESG	Non	Non	−5.7	8	9	454.4	Y -ESG
YSIL	Non	Non	−2.14	7	7	494.6	Y-SI-L
AEMPP	Non	Allergen	−4.96	5	8	543.6	Good
AEQEK	Non	Non	−8.71	10	11	603.6	Good
AINPY	Non	Allergen	−3.02	7	8	576.6	Good
AKEHF	Non	Allergen	−5.69	9	9	630.7	AK-EH-F
ASKQK	Non	Non	−6.70	10	8	560.6	ASK-QK
AYKKL	Non	Non	−3.64	9	7	621.8	AY-K-K-L

CEQMR	Non	Non	−5.95	10	9	665.8	CEQ-M-R
CIEAH	Non	Allergen	−3.52	8	9	571.6	Good
CINYT	Non	Non	−4.41	9	9	612.7	CINY-T
DNQIK	Non	Allergen	−8.76	10	10	616.7	DNQI-K
EEVQK	Non	Allergen	−7.75	10	10	631.7	Good
EKKIR	Non	Non	−6.78	11	8	672.8	EK-K-IR
EMKWK	Non	Allergen	−5.52	10	8	720.9	EM-K-W-K
ENAQK	Non	Allergen	−9.72	10	10	588.6	Good
EPIVK	Non	Allergen	−6.16	7	8	584.7	Good
EQEEY	Non	Non	−7.19	11	14	696.7	Good
HIKEL	Non	Non	−4.63	9	9	638.8	H-IK-E-L
HKESL	Non	Allergen	−7.00	10	10	612.7	H-K-ESL
IKKKL	Non	Non	−2.44	9	6	628.8	IK-K-K-K-L
KIKVG	Non	Non	−3.31	8	6	543.7	K-IK-VG
KKKKG	Non	Non	−5.36	10	6	587.8	K-K-K-K-G
KNPMF	Non	Non	−3.23	7	7	635.8	K-NPM-F
KNYER	Non	Non	−8.15	12	10	708.8	K-NY-ET
NCWVP	Non	Non	−2.37	7	7	617.7	NCW-VP
NHHMF	Non	Non	−3.77	9	9	684.8	NH-H-M-F
NKVKP	Non	Allergen	−6.42	8	7	584.7	NK-VKP
NYHIF	Non	Non	−1.62	9	9	692.8	NY-H-I-F
PPEPDT	Non	Allergen	−5.07	8	11	557.6	Good
QDHEN	Non	Non	−8.31	11	13	641.6	QDH-EN
QEQDH	Non	Allergen	−7.95	11	13	655.6	Good
QESKT	Non	Allergen	−9.87	10	10	591.6	QESK-T
QKNDL	Non	Allergen	−8.76	10	10	616.7	QK-NDL
QMNPP	Non	Allergen	−5.44	6	8	585.7	QM-NPP
QVKEL	Non	Allergen	−7.50	9	9	615.7	QVK-E-L
SKVEK	Non	Non	−7.36	10	9	589.7	SK-VEK
VDKYR	Non	Non	−6.02	11	9	679.8	VDK-Y-R
VQQEL	Non	Non	−6.61	9	10	615.7	VQQ-E-L
YDNHL	Non	Allergen	−4.08	10	11	660.7	Y-DNH-L
ADIKEL	Non	Allergen	−5.52	10	11	687.8	ADIK-E-L
AEMPPH	Non	Allergen	−3.76	7	10	680.8	Good
AINPYR	Non	Allergen	−3.75	10	9	732.8	AINPY-R
AVPDPG	Non	Allergen	−3.96	6	9	554.6	Good
CIAINP	Non	Non	−2.92	7	8	629.8	Good
DQIDQL	Non	Allergen	−5.88	11	13	730.8	Good
IIYSEF	Non	Allergen	−0.70	9	9	754.9	IIY-SE-F
NKVKPL	Non	Allergen	−5.18	9	8	697.9	NK-VKP-L
QCNPVL	Non	Allergen	−6.14	8	9	672.8	Good
QKVKSR	Non	Non	−5.41	12	9	687.8	QK-VK-SR
QMNPPK	Non	Non	−5.93	8	9	713.8	QM-NPPK

Table S6 Predicted toxicity, allergenicity, and intestinal epithelial permeability of newly formed peptides by gastrointestinal proteases

Peptide	Toxicity	Allergenicity	CLog*P*	H-bond donors	H-bond acceptors	MWT
ADIK	Non	Allergen	−6.01	7	7	445.5
AE	Non	Allergen	−3.76	4	5	218.2
AK	Non	Non	−3.49	4	3	217.3
ASK	Non	Non	−5.23	6	5	304.3
CEQ	Non	Non	−5.37	6	7	378.4
CINY	Non	Non	−2.61	7	7	511.6
DNH	Non	Non	−6.13	7	8	384.3
DNQI	Non	Allergen	−6.18	8	9	488.5
EH	Non	Allergen	−4.35	5	6	284.3
EM	Non	Allergen	−3.70	4	5	278.3
EN	Non	Allergen	−5.28	5	6	261.2
EP	Non	Allergen	−3.59	3	5	244.2
ESG	Non	Allergen	−5.47	6	7	291.3
ESL	Non	Non	−4.18	6	7	347.4
ET	Non	Allergen	−4.38	5	6	248.2
IIY	Non	Non	−1.41	5	5	407.5
IK	Non	Allergen	−3.27	4	3	259.3
NCW	Non	Non	−4.06	6	5	421.5
NDL	Non	Non	−4.31	6	7	360.4
NH	Non	Non	−5.36	5	5	269.3
NPM	Non	Non	−5.08	4	5	360.4
NPP	Non	Allergen	−4.42	3	5	326.3
NPPK	Non	Non	−4.91	5	6	454.5
NR	Non	Allergen	−5.59	6	4	288.3
PIY	Non	Allergen	−1.58	5	5	391.5
QDH	Non	Non	−5.77	7	8	398.4
QESK	Non	Allergen	−9.00	9	9	490.5
QM	Non	Non	−4.35	4	4	277.3
QQK	Non	Allergen	−6.07	7	6	402.4
QVK	Non	Allergen	−5.61	6	5	373.4
QY	Non	Non	−4.42	5	5	309.3
SE	Non	Allergen	−4.32	5	6	234.2
SI	Non	Non	−3.65	4	4	218.3
SK	Non	Allergen	−4.05	5	4	233.3
SR	Non	Allergen	−4.63	6	4	261.3
VDK	Non	Non	−5.93	6	6	360.4
VEK	Non	Non	−5.57	6	6	374.4
VKP	Non	Allergen	−3.49	4	4	342.4
VQQ	Non	Non	−6.54	6	6	373.4
VT	Non	Allergen	−3.66	4	4	218.3

Figure S1 Nine new ACE inhibitory peptides located in myosin heavy chain of *Todarodes pacificus*

1 MSSYDPSDPDMEFLCLTRQRQLEITTVPFDGKKNCWVPDPEQGFVSAEIQSTKGDEVTVK
61 TDKSMEMRTVKKDDVG | **QM** | **NPPK** | FEMNMDMANLTFLNEA | **SI** | LHNLRSRYESGFIYTYSGLF
121 CIAINPYRRLPIYTQGLVDKYRGKRRAEMPPHLF | **SI** | ADNAY | **QY** | MLQDHENQSMLITGESG
181 AGKTENTKKVI | **QY** | FALVAASLTSGGKDKKKEEEKKKDEKKGTLEDQIVQCNPVLEAYGNA
241 KTTRNNNSSRFGKFIRIHFGTQGKIAGADIETYLLEKSRVTYQQSAERNYHIFYQLLSPA
301 FPANIEKILAVPDPGLYGFINQGHLSVDGIDDEEEMQLTDTAFDVLGFTDDEKLSMYKCT
361 GCILHLGEMKWKQRGEQAEADGTAEAEKVAFLLGVNAGDLLKCLLKPKIKVGTEYVTQGR
421 NKDQVSN | **SI** | AAL | **AK** | SLYDRMFNWLVKRVNTTLDTK | **AK** | RQFFIGVLDIAGFEIFDYNSFEQ
481 LCINYTNERLQQFF | **NH** | HMFVLEQEEYKKEGIVWEFIDFGLDLQACIELIEKPMGIL | **SI** | LE
541 EECMFPKASDLSFKNKLYD | **NH** | LGK | **NPM** | FGKPKPPKAGCIEAHFALHHYAGSVSYNISSWL
601 EKNKDPINENVVELLQTSKEPIVKMLFTPPEDTSPAGGKKKKGKSAAFQTISSTHKESLN
661 KLMKNLYSTHPHFVRCIIPNELKTPGMIDAALVLHQLRCNGVLEGIRICRKGFPNR | **IIY** | S
721 EFKQRY | **SI** | LAP | **NAIP** | SGFADGKVVTDKVLSALQLDTNEYRLGNTKVFFKAGVLGMLEDMR
781 DERLSKIISMFQAHIRGYLMRKAYKKLQDQRIGLTLIQRNIRKWLMLRNWEWWRLFNKVK
841 PLLGMARQEEENKKAAEEF | **AK** | MKEEFLRCE | **QM** | RKELEEQNTVLMQQKNDLVISMSSSDDA
901 IIESEEKIEGLIKQKSDMETHIKELEEKLMDEEDAATDLAA | **AK** | KKSEADIKELKQDVEDL
961 EAGL | **AK** | AEQEKTTKDNQIKTLQDEMANQDEALSKVNKEKKALEEVQKKTLEDLQAEEDKV
1021 | **NH** | LSKLKTKLEQTLDELEDNLEREKKIRADVDK | **AK** | RKVEQDLKTTQETVEDLERVKRDLE
1081 DAGRKKDMEINGLNSKLEDEQNLVAQLQKKIKELQARIEELEEELEAERQARSKVEKQRT
1141 ELSREMEELGERLDEAGGATAA | **QM** | ELNKKREQELLRLRRDLEENTMQNESTIATLRKKNQ
1201 EATNELGDQIDQLQKVKSRLEKEKNELKEKAEEAMMELKHREKNMGCSEKMSK | **QM** | EAQLS
1261 ELNGKIDEQAR | **SI** | SELGSQKSRLQVEAADLTRQLEEAEHNVGQLTKLKSSMGVNLED | **AK** | R
1321 SLEDEARLR | **AK** | LQAEVRNLNSDIDGIRESLEEEQESKTDLQRALSRANAEVQQWRSKFES
1381 EGAARADELYDSKRKLQAELSEAEQTADTLHSKCAALEK | **AK** | SRLQGELEDLAIDAERSSA
1441 HANNLEKKQRNFDKVVSEWQHKCNDLQAELENAQKEARSYSAELFRVRAQCEEVGDTVES
1501 LRRENKNLADEIHDLTDQLGEGGRSTHELEKARKRLALEKEELQAALEEAEAALEQEE | **AK** |
1561 VMRATLEISQIRQEIDRRLQEKEEEFDNTRR | **NH** | QRAIESMQASLEAE | **AK** | GKAEALRIKKK
1621 LEGDINELEIALDATNRGKAELEKNVKKYQGQIRELQSAVEEEQRQRDE | **AK** | EHFMMAERR
1681 CAAINGELEELRTILEQAERARKAAENELADASDRVNELTAQVSTSNSQKRKLEGDVTAM
1741 QSDLDELNNELKDADDR | **AK** | HAMGDATRLADELRQEQDHGL | **SI** | EKMRKSLESQVKELQVRL
1801 DESEAAALKGGKKMIQKLESRVRELEAELDSEQRRHAETQKSMRKVDRRVKELSFQQEED
1861 RKNYERMQELVDKLQNKIKTYKRQVEEAEEIAAINL | **AK** | FRKVQQELEDAEERADQSEGAL
1921 QKLR | **AK** | NRSSVSVARTSPM
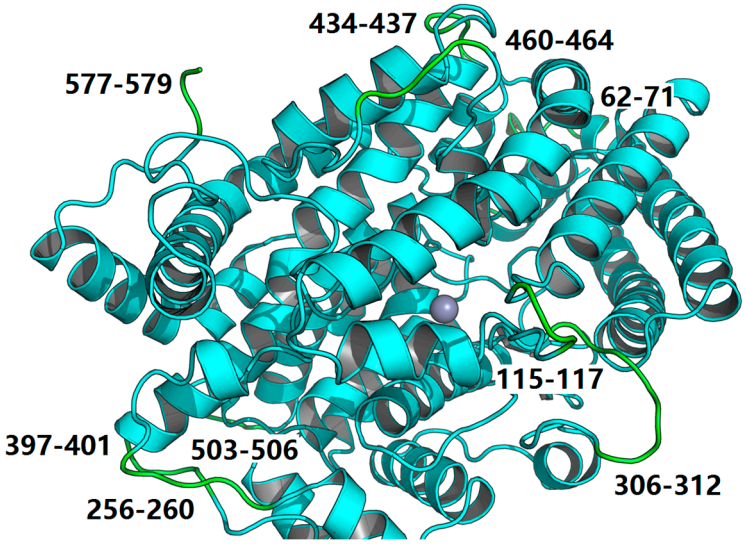
Figure S2 Regional flexibility (green) of ACE with and without peptides Ile-Ile-Tyr and Asn-Pro-Pro-Lys during molecular dynamics simulation.